5-2019

Minocycline inhibits PDGF-BB-induced human aortic smooth muscle cell proliferation and migration by reversing miR-221- and -222-mediated RECK suppression

Yusuke Higashi

Srinivas Mummidi

Sergiy Sukhanov

Tadashi Yoshida

Makoto Noda

See next page for additional authors

Authors

Yusuke Higashi, Srinivas Mummidi, Sergiy Sukhanov, Tadashi Yoshida, Makoto Noda, Patrice Delafontaine, and Bysani Chandrasekar

Minocycline Inhibits PDGF-BB-induced Human Aortic Smooth Muscle Cell Proliferation and Migration by reversing miR-221- and -222-mediated RECK suppression

Yusuke Higashi,[1,2,§] Mummidi Srinivas,[3,§] Sergiy Sukhanov, [1,2] Tadashi Yoshida, [1,2]

Makoto Noda,[4] Patrice Delafontaine, [1] Bysani Chandrasekar[1,2,5,6,*]

[1]Medicine/Cardiovascular Medicine, University of Missouri School of Medicine, Columbia, MO, USA

[2]Department of Medical Pharmacology and Physiology, University of Missouri School of Medicine, Columbia, MO, USA

[3]Department of Human Genetics and South Texas Diabetes and Obesity Institute, The University of Texas Rio Grande Valley School of Medicine, Edinburg, TX, USA

[4]Department of Molecular Oncology, Kyoto University Graduate School of Medicine, Sakyo-ku, Kyoto 606-8501, Japan

[5]Research Service, Harry S. Truman Memorial Veterans' Hospital, Columbia, MO, USA

[6]Dalton Cardiovascular Research Center, University of Missouri, Columbia, MO, USA

§Equal contribution

Running title: Minocycline, RECK and smooth muscle cell proliferation and migration

*To whom correspondence should be addressed: Bysani Chandrasekar, DVM. Ph.D., Medicine/Cardiovascular Medicine, University of Missouri School of Medicine, 1 Hospital Drive, Columbia, MO 65212, Phone: 573-882-8450, Fax: 573-884-7743, E-mail: chandrasekarb@health.missouri.edu

Abstract

Minocycline, a tetracycline antibiotic, is known to exert vasculoprotective effects independent of its anti-bacterial properties; however the underlying molecular mechanisms are not completely understood. Reversion Inducing Cysteine Rich Protein with Kazal Motifs (RECK) is a cell surface expressed, membrane anchored protein, and its overexpression inhibits cancer cell migration. We hypothesized that minocycline inhibits platelet-derived growth factor (PDGF)-induced human aortic smooth muscle cell (SMC) proliferation and migration via RECK upregulation. Our data show that the BB homodimer of recombinant PDGF (PDGF-BB) induced SMC migration and proliferation, effects significantly blunted by pre-treatment with minocycline. Further investigations revealed that PDGF-BB induced PI3K-dependent AKT activation, MEK-dependent ERK activation, reactive oxygen species generation, Nuclear Factor-κB and Activator Protein-1 activation, microRNA (miR)-221 and miR-222 induction, RECK suppression, and matrix metalloproteinase (MMP2 and 9) activation, effects that were reversed by minocycline. Notably, minocycline induced RECK expression dose-dependently within the therapeutic dose of 1-100 μM, and silencing RECK partially reversed the inhibitory effects of minocycline on PDGF-BB-induced MMP activation, and SMC proliferation and migration. Further, targeting MMP2 and MMP9 blunted PDGF-BB-induced SMC migration. Together, these results demonstrate that minocycline inhibits PDGF-BB-induced SMC proliferation and migration by restoring RECK expression and inhibiting MMP activation. These results indicate that the induction of RECK is one of the mechanisms by which minocycline exerts vasculoprotective effects.

Keywords: Vascular Proliferative diseases, restenosis, mitogenesis, migration, PDGF, RECK, MMP

1. Introduction

Dysregulated proliferation and migration of arterial smooth muscle cells lead to vascular complications, including intimal hyperplasia. Among various growth factors, the Platelet-derived growth factor (PDGF) family exerts potent mitogenic and migratory effects on vascular smooth muscle cells, ultimately resulting in intimal hyperplasia [1, 2]. There are four members in PDGF family, PDGF-A, -B, -C and –D, that dimerize and signal via PDGF receptors alpha and beta. Both PDGFRα and PDGFRβ are class III receptor tyrosine kinases, and form either homo or heterodimers depending upon ligand binding [3]. Among various homo- or heterodimers of members of the PDGF family, the PDGF-BB homodimer appears to be highly potent in exerting mitogenic and migratory effects [3] via activation of multiple kinase-dependent signaling cascades, including activation of PI3K/AKT and mitogen activated protein kinases [4, 5]. Furthermore, a significant role for oxidative stress and oxidative stress-sensitive NF-κB (nuclear factor kappa-light-chain-enhancer of activated B cells)-dependent signaling and its downstream effectors microRNA (miR)-221 and miR-222 have also been implicated. However, the potential targets of these miRs in the context of human arterial smooth muscle proliferation and migration have yet to be fully identified.

Minocycline (7-dimethylamino-6-dimethyl-6-deoxytetracycline) is a US Food and Drug Administration (FDA)-approved second-generation, semi-synthetic, orally active tetracycline antibiotic. However, its antibiotic-independent effects have also been described, including vasculoprotection. In fact, minocycline has been shown to inhibit vascular endothelial growth factor (VEGF)-induced aortic smooth muscle cell (SMC) migration by suppressing ERK (Extracellular Signal-Regulated Kinase)- and PI3K (Phosphoinositide 3-Kinase)/AKT (V-Akt Murine Thymoma Viral Oncogene Homolog)-dependent signaling and matrix metallopeptidase

(MMP)-9 induction [6]. In fact, in a rat model of balloon injury, minocycline blunted neointima formation by inhibiting MMP expression and SMC migration [6, 7]. Furthermore, minocycline reduced atherosclerotic plaque size in apolipoprotein E-deficient mice, a murine model of atherosclerosis, via a PARP1 (Poly[ADP-Ribose]Polymerase 1) and p27Kip1-dependent suppression of SMC proliferation [8]. These reports suggest that minocycline may have therapeutic potential in vascular proliferative diseases.

RECK (Reversion Inducing Cysteine Rich Protein with Kazal Motifs) is first described as a tumor suppressor gene [9-12]. It is a glycosylphosphatidylinositol (GPI) anchored membrane protein known to inhibit secretion and activation of MMPs. It is expressed in various cell types, including adipocytes, vascular endothelial cells, smooth muscle cells, cardiomyocytes and cardiac fibroblasts [13]. We have previously reported that ectopic expression of RECK suppresses angiotensin II-mediated cardiac fibroblast migration in vitro and cardiac fibrosis in vivo [14-16].

Many types of cancer cells express low levels of RECK, possibly contributing to their malignant potential. Supporting this hypothesis, forced expression of RECK has been shown to suppress cancer cell migration and proliferation [17, 18], suggesting that RECK inducers may have therapeutic potential in lowering tumor growth, malignancy and metastasis. In an attempt to identify small compounds that can induce *Reck* gene expression, Noda et al. have identified minocycline as a potent activator of RECK promoter activity using a reporter gene assay in RAS-transformed fibroblasts [19]. Here, we hypothesized that by upregulating RECK, minocycline inhibits PDGF-induced human ASMC (SMC) proliferation and migration. Our results show that PDGF-BB differentially regulates RECK and MMPs; suppresses RECK, but induces MMPs activation; resulting ultimately in increased SMC proliferation and migration.

Further supporting our hypothesis, minocycline reversed PDGF-BB-induced RECK suppression and inhibited SMC proliferation and migration. To our knowledge, this is the first report demonstrating the role of RECK in minocycline-induced suppression of PDGF-mediated SMC proliferation and migration. Our data suggest a possible therapeutic role for minocycline and other RECK inducers in vascular proliferative diseases.

2. Materials and methods

2.1. Materials

Carrier-free recombinant human PDGF-BB protein was obtained from R&D Systems (#220-BB; Minneapolis, MN). The gp91 ds-tat (*YGRKKRRQRRRCSTRIRRQL - NH2*; #AS-63818) and its scrambled peptide control sgp91 ds-tat (*YGRKKRRQRRRCLRITRQSR - NH2*; #AS-63821) were purchased from AnaSpec (Fremont, CA, USA). One of the major sources of superoxide generation is NADPH oxidase (NOX). SMC express Nox2 ($gp91^{phox}$) along with its cell membrane and cytosolic components [20]. Binding of $gp91^{phox}$ to the p47-p67-$p40^{phox}$ complex is critical in activation of Nox2. A specific gp91 docking sequence (ds in gp91 ds, blue) which is responsible for binding of $gp91^{phox}$ and $gp47^{phox}$ is linked to a specific 9-amino acid peptide of HIV (Human Immunodeficiency Virus) viral coat (HIV-tat, red), resulting in gp91 ds-tat which is used previously to block their interaction to disrupt Nox2 assembly and function. A scrambled sequence linked to HIV-tat served as a control (sgp91 ds-tat) [20]. The Nox1/Nox4 inhibitor GKT137831 (2-2(chlorophenyl)-4-[3-(dimethylamino) phenyl]-5-methyl-1H-pyrazolo[4,3-c]pyridine-3,6(2H,5H)-dione; #17164) was purchased from Cayman Chemical (Ann Arbor, MI). Minocycline (#9511), N-acetyl-L-cysteine (NAC; #A7250), cell culture supplies, cOmplete™ Protease Inhibitor Cocktail (#11697498001), PhosSTOP™ (#4906845001), Trypsin-EDTA solution (#T4049), Trypan Blue solution (#T8154), Dimethyl Sulfoxide (DMSO, #D8418) and all other chemicals were purchased from Sigma-Aldrich (St. Louis, MO). The PI3K inhibitor Wortmannin (#S2758, 100 nM in DMSO for 1h), the AKT inhibitor MK-2206 2HCl (#S1078; a highly selective orally active pan-AKT inhibitor with no inhibitory activities against 250 other protein kinases, 5μM for 1h), and the ERK inhibitor SCH772984 (#S7101; a novel, specific inhibitor of ERK1/2, 10μM in DMSO for 1 h) were purchased from Sellechem

(Houston, TX). Restore™ Western blot Stripping Buffer (#21059), CyQUANT® Cell Proliferation Assay (#C7026), Vybrant® MTT (3-(4,5-dimethylthiazol-2-yl)-2,5-diphenyltetrazolium bromide) Cell Proliferation Assay Kit (#V13154), Amplex® Red Hydrogen Peroxide/Peroxidase Assay Kit (#A22188), and Corning® BioCoat™ Matrigel® Migration Chambers with 8.0μm polyethylene terephthalate (PET) membrane (#11563570) were purchased from Thermo Fisher Scientific. Cell Death Detection ELISA^{PLUS} kit (#11774425001) was purchased from Roche Life Science (Indianapolis, IN). Human RECK (NM_021111; ~1.5 kb) 3'-UTR (untranslated region) clone in pMirTarget vector was purchased from Origene (#SC214511, Rockville, MD). QuikChange II Site-Directed Mutagenesis Kit (#2000523) was purchased from Agilent Technologies/Stratagene (Santa Clara, CA). Dual-Luciferase® Reporter Assay System (#E1910) was purchased from Promega (Madison, WI). 96-well clear bottom, black-sided plates (#29444-008) were purchased from VWR Scientific (West Chester, PA). Polybrene® (sc-134220) was purchased from Santa Cruz Biotechnology, Inc. At the indicated concentrations and for the duration of treatment, the pharmacological inhibitors failed to modulate SMC morphology, viability or adherence to culture dishes (data not shown).

2.2. Cell culture-normal human aortic SMC

Normal human aortic smooth muscle cells (T/G HA-VSMC; SMC) were purchased from ATCC (#CRL-1999, Manassas, VA, USA). The cells were authenticated by the vendor for sterility (aerobic and anaerobic) and were pathogen-free. The cells were grown as previously described [21] in Ham's F12 medium supplemented with 10% (vol/vol) FBS and endothelial cell growth supplement (0.03 mg/ml). At 70–80% confluency, the complete medium was replaced with Ham's F12/0.5% BSA. After 48 h, the quiescent SMC were incubated with PDGF-BB (10

ng/ml) for the indicated time periods. At the end of the experimental period, cells were harvested, snap frozen, and stored at −80°C. All other treatment conditions are detailed below and in figure legends.

2.3. Adeno- and Lentiviral transduction

The following lentiviral shRNA vectors against IKKβ (#sc-35645-V), p65 (#sc-29410-V), JNK2 (#sc-39101-V), and c-Jun (#sc-29223-V) were purchased from Santa Cruz Biotechnology, Inc. Lentiviral shRNA against RECK (SHCLNV-NM_021111; TRCN0000376461) and eGFP (SHC005V) were purchased from Sigma-Aldrich. All lentiviral vectors are previously described [22, 23]. For lentiviral infection, SMC at 50–60% confluency were infected with the indicated lentiviral shRNA at a multiplicity of infection (moi) of 0.5 for 48 h in complete media. To increase infection efficiency, cells were co-treated with the cationic polymer Polybrene® (5 μg/ml in water). Neither shRNA nor Polybrene affected cell viability. The following adenoviral vectors were used: RECK (Ad.RECK), MMP2 siRNA (Ad.siMMP2), MMP9 siRNA (Ad.siMMP9), siGFP (Ad.siGFP), and eGFP (Ad.eGFP). All adenoviral vectors are previously described [24, 25]. At ~70% confluency, CF were infected at ambient temperature with adenoviruses in PBS at the indicated moi. After 1 h, the medium containing adenovirus was replaced with fresh culture medium. Assays were carried out after 24h (RECK, eGFP) or 48h (siMMP2, siMMP9, sieGFP). At the indicated moi and for the duration of treatment, adenoviral vectors had no off-target effects, and failed to modulate SMC adherence, shape or viability (trypan blue-dye exclusion; data not shown).

2.4. miRNA expression, inhibitors and transfections

For miRNA expression, small RNA-enriched total RNA was isolated using the *mir*Vana™ miRNA Isolation Kit (Ambion®). Expression of human miR-221 (477981-mir) and miR-222 (477982-mir) was analyzed using TaqMan® Advanced miRNA assays (Thermo Fisher Scientific). U6 served as a loading control. Relative expression levels of microRNAs were calculated using the $2^{-\Delta\Delta Ct}$ method. Human miR-221 (has-miR-221, Assay ID: MH10337; #4464084) -222 (Assay ID: MC11376; #4464066) inhibitors and an inhibitor control (Anti-miR™ miRNA inhibitor negative control#1, #AM17010) were also purchased from Thermo Fisher Scientific. SMC were transfected with the inhibitor or the inhibitor control (80 nM) as previously described [16] using the Neon® transfection system (MPK-5000, Invitrogen) with the following parameters: pulse voltage: 1300 volts, pulse width: 20 ms, pulse number: 2, and the tip type: 10 µl, and then cultured for 24 h. SMC showed transfection efficiency of 51% with only 6% cell death as determined using the pEGFP-N1 vector. Transfections at the indicated concentration and for the duration of treatment failed to significantly modulate SMC adherence, shape or viability (trypan blue-dye exclusion; data not shown).

2.5. *RECK* 3'UTR analysis

Human *RECK* 3'UTR sequence was amplified and subcloned into pMIR-REPORT vector (The Ambion® pMIR-REPORT™ miRNA Expression Reporter Vector System). Mutations in miR-221/222 binding site (-AUGUAGC- to -UACAUCG-) [26] were introduced by site-directed mutagenesis using the QuikChange II Site-Directed Muatagenesis Kit as previously reported [16] and confirmed by nucleotide sequencing. SMC were transfected with the wild type (WT, *RECK*-3'UTR) or mutant (m*RECK*-3'UTR) *RECK* pMIR-REPORTER vectors using the Neon®

transfection system as described above with 3 µg of plasmid DNA for 24 h, co-transfected with the *Renilla* luciferase vector (pRL-TK, 100 ng) prior to PDGF-BB addition (10 ng/ml for 12 h), and analyzed for reporter activity using the Dual-Luciferase® Reporter Assay System, and the results are presented as a ration of Firefly luciferase activity to that of corresponding *Renilla* luciferase activity.

2.6. Superoxide and hydrogen peroxide production

Superoxide ($O_2^{-\bullet}$) generation was quantified using the lucigenin-enhanced chemiluminescence assay as previously described [24, 27]. After subtracting background luminescence, results are expressed as pmol superoxide/min/mg protein. Studies were also performed after treating cells with the Nox2 inhibitor gp91ds-tat (1 µM for 1 h). A corresponding scrambled peptide served as a control. Hydrogen peroxide (H_2O_2) production was measured according to the manufacturer's instructions using a commercially available kit in the presence of horseradish peroxidase (0.1 unit/ml, Amplex Red: and 50 µM) as has been previously described [27]. Fluorescence was recorded at 530 nm excitation and 590 nm emission wavelengths (CytoFluor II; Applied Biosystems, Foster City, CA). Standard curves were generated using known concentrations of H_2O_2. Studies were also performed after treatment with the Nox1/4 dual inhibitor GKT137831. The results are expressed as µM H_2O_2 produced/10^6 cells.

2.7. Immunoblotting and activity assays

Preparation of whole cell homogenates, immunoblotting, detection of the immuno-reactive bands by enhanced chemiluminescence, and quantification by densitometry are all

described previously [24, 27]. Immunoblotting was performed at least three separate occasions (biological and not intra-assay variables), and a representative immunoblot is shown in the figures. The source and concentration of antibodies used in immunoblotting are as follows: AKT (#4685, 1:1000; Cell Signaling Technology, Inc/CST), phospho-AKT (Ser^{473}; #4060, 1:1000, CST), ERK (#9102, 1:1000, CST), phospho-ERK (Thr^{202}/Tyr^{204}; #9101, 1:1000, CST), Tubulin (#2144, 1:1000, CST), phospho-c-Jun (Ser63; #9261, 1:1000, CST), c-Jun (#9165, 1:1000, CST), IKKβ (#2370, 1:1000, CST), phospho-p65 (#3033, 1:1000, CST), p65 (#3034, 1:1000, CST), RECK (#3433, 1:1000, CST), cleaved caspase-3 (#9664, 1μg/ml, CST), JNK2 ab178953, 1:1000, abcam), caspase-3 (ab32499; 1:5000; abcam), MMP2 (detects both pro and active forms; #AB19016, 1:2000, Millipore-Sigma), MMP2 (detects only the pro-form, #MAB13405, 0.5 μg/ml, Millipore-Sigma), MMP9 (detects both pro and active forms; #MAB3309, 1:2500, Chemicon, Temecula, CA), and MMP9 (detects only the pro-form; MAB9111-SP; R&D Systems, Minneapolis, MN).

2.8. Transwell migration assays

SMC migration was quantified using the Discovery Labware BD BioCoat™ Matrigel™ invasion chambers (Cat. #354481, BD Biosciences) and 8.0-μm pore PET membranes with a thin layer of Matrigel™ basement membrane matrix. Cultured SMCs were trypsinized and suspended in Ham's F12 medium and 0.5% BSA, and 1 ml containing 2.0×10^5 cells/ml was layered on the coated insert filters. Cells were stimulated with PDGF-BB (10 ng/ml). The lower chamber contained 20% FBS. After incubation at 37°C for 18 h, the membranes were removed and washed with PBS, and the non-invading cells on the upper surface were removed with a cotton swab. The cells migrating to the lower surface of the membrane were quantified using the MTT

assay. In a subset of experiments, the layered cells were incubated with NAC, gp91 ds-tat, GKT137831, minocycline, inhibitors of miR221, miR-222, lentiviral shRNA against RECK, or respective controls prior to PDGF-BB addition.

2.9. Cell proliferation

The effects of PDGF-BB on SMC proliferation were analyzed according to manufacturer's protocol using the CyQUANT® assay. Briefly, SMC were plated at $2x10^3$ cells per well into 96-well clear bottom, black-sided plates, and allowed to attach overnight. After 24 h, the cells were fed with serum-free medium containing 0.5% BSA and incubated for an additional 24 h. Cells were then continuously stimulated with PDGF-BB (10 ng/ml) in serum-free medium for 48 h. After removing the medium, the plates were frozen at −80 °C for 2 h before assay. Plates were then thawed, stained with CyQUANT® GR dye according to manufacturer's protocol, and assayed on a FLX800 microplate fluorescence reader (Bio-Tek Instruments, Winooski, VT) using 485/20 excitation and 528/20 emission filters, and analyzed using KC4 software (Bio-Tek). Proliferation assays were carried out 6 times. To determine the role of oxidative stress, miR-221, miR-222 and RECK, SMC were incubated with NAC, gp91 ds-tat, GKT137831, minocycline, inhibitors of miR-221, miR-222, lentiviral shRNA against RECK, adenoviral vectors expressing MMP2 and MMP9 silencing RNA, or respective controls prior to PDGF-BB addition.

2.10. Cell death assays

To investigate whether minocycline induces cell death, SMC were cultured in complete medium until ~70% confluent. The medium was replaced with Ham's F12 medium with 0.5%

BSA, and incubated for 48 h. Minocycline was added at the indicated doses, and analyzed for cell death after 8 h by determining pro-caspase-3 (~35 kDa) and active-caspase-3 (~17/19 kDa) levels by immunoblotting. As a positive control, H_2O_2 was added to a final concentration of 100 μM.

2.11. Statistical Analysis

Comparisons between controls and various treatments were performed by ANOVA with post hoc Dunnett's *t*-tests. All assays were performed at least three times, and the error bars in the figures indicate the S.E. Though a representative immunoblot is shown in the main figures, changes in protein/phosphorylation levels from three independent experiments were semi-quantified by densitometry, and were shown as ratios and fold changes from untreated or respective controls whenever the results are less clear.

3. Results

3.1. Minocycline inhibits PDGF-BB-mediated PI3K/AKT- and ERK-dependent SMC migration and proliferation without affecting cell viability.

Multiple signal transduction pathways are implicated in PDGF-induced SMC proliferation and migration, including AKT and ERK activation. Therefore, we investigated whether PDGF-BB induces SMC migration and proliferation via AKT and ERK activation, and whether minocycline blunts these responses. Indeed, PDGF-BB induced time dependent AKT activation, as evidenced by the increased levels of phosphor-AKT (Ser^{473}) levels (Fig. 1A), an effect inhibited by the PI3K inhibitor Wortmannin, the AKT inhibitor MK2206, and mionocycline (Fig. 1B). Moreover, pre-treatment with Wortmannin, MK2206 and minocycline each attenuated PDGF-BB-induced SMC migration (Fig. 1C) and proliferation (Fig. 1D) without affecting cell viability (Fig. 1D, inset). However, hydrogen peroxide, used as a positive control, induced cell death, as evidenced by increased levels of cleaved caspse-3 levels (Fig. 1D, inset). Similarly, PDGF-BB induced time-dependent ERK activation, as evidenced by the increased levels of phospho-ERK levels (Fig. 2A), an effect blunted by the ERK inhibitor SCH772984 and minocycline. Further, inhibiting ERK activation attenuated PDGF-BB-induced SMC migration (Fig. 2C) and proliferation (Fig. 2D), and without affecting cell viability (Fig. 2D, inset). Hydrogen peroxide, used as a positive control, did induce cell death, as evidenced by increased levels of cleaved caspse-3 levels (Fig. 2D, inset). Together, these results indicate that (i) PDGHF-BB induces SMC migration and proliferation in part via AKT and ERK, and (ii) pretreatment with minocycline inhibits AKT and ERK activation, and SMC migration and proliferation, without affecting cell viability (Fig. 1 and Fig. 2).

3.2. Minocycline inhibits PDGF-BB-induced reactive oxygen species generation and redox-sensitive SMC migration and proliferation

PDGF-BB has been shown to induce oxidative stress in various cell types. Since minocycline exerts antioxidant effects, we next investigated whether PDGF-BB-mediated SMC migration and proliferation is redox-sensitive manner, and whether minocycline blunts this response. Indeed, PDGF-BB significantly increased superoxide generation, an effect markedly attenuated by the broad- spectrum antioxidant NAC and the Nox2 inhibitor gp91 ds-tat (Fig. 3A). PDGF-BB also stimulated hydrogen peroxide generation, an effect inhibited by NAC as well as the Nox1/4 dual inhibitor GKT137831 (Fig. 3B). Furthermore, all three antioxidants, i.e., NAC, gp91 ds-tat, and GKT137831, inhibited SMC migration and (Fig. 3C) and proliferation (Fig. 3D), without affecting cell viability (Fig. 3E). Importantly, minocycline inhibited PDGF-BB-induced superoxide and hydrogen peroxide (Fig. 3A, 3B). Together these results indicate that minocycline blunts PDGF-BB-induced SMC migration and proliferation by inhibiting oxidative stress (Fig. 3A).

The redox-sensitive nuclear transcription factors NF-κB and AP-1 (Activator Protein-1) are essential mediators of PDGF signaling [28, 29]. Our data show that treatment with PDGF-BB activated both transcription factors in a time-dependent manner, as evidenced by the increased levels of phospho-p65 (Ser^{536}) (Fig. 4A) and phospho-c-Jun (Ser^{63}) (Fig. 4B). Since IKK and JNK are upstream of NF-κB and AP-1, we next investigated whether silencing IKK and JNK attenuate their activation. Indeed, while silencing IKKβ inhibited PDGF-BB-induced p65 phosphorylation (Fig. 4C), knockdown of JNK2 attenuated c-Jun phosphorylation (Fig. 4D). Importantly, pretreatment with minocycline inhibited activation of both NF-κB and AP-1 (Fig.

4C and 4D), consistent with its antioxidant effects and eventual inhibition of PDGF-BB-induced NF-κB and AP-1 activation (Fig. 4).

3.3 PDGF-BB induces SMC migration and proliferation via IKK/NF-κB- and JNK/AP-1-dependent miR-221 and miR-222 induction

Multiple microRNAs, including miR221 and miR-222, are shown to regulate PDGF-induced SMC migration and proliferation [30, 31]. Since both NF-κB and AP-1 regulate the miR-221 and miR-222 induction, we next determined whether silencing targeting IKK/NF-κB and JNK/AP-1 will inhibit their expression, and whether targeting miR-221 and miR-222 will blunt PDGF-BB-induced SMC migration and proliferation. Results show that silencing IKKβ, p65, JNK2 and c-Jun, each attenuated PDGF-BB-induced miR-221 (Fig. 5A) and miR-222 (Fig. 5D) expression. Further, the inhibitors of miR-221 and miR-222 each attenuated PDGF-BB-induced SMC migration (Fig. 5C) and proliferation (Fig. 5D), with affecting cell viability (Fig. 5E). Together, these data demonstrate that PDGF-BB induces SMC migration and proliferation in part via IKK/NF-κB- and JNK/AP-1-dependent miR-221 and miR-222 induction (Fig. 5).

3.4. Targeting miR-221 and miR-222 reverses PDGF-BB-induced RECK suppression

We and others have previously demonstrated that the membrane-anchored MMP inhibitor RECK is a potent inhibitor of cell migration [14, 15, 24, 26]. Therefore, we sought out to determine the potential link between PDGF-BB, RECK, and miRs 221 and 222 in SMC. The results show that SMC express RECK at basal conditions, and treatment with PDGF-BB suppressed its expression (Fig. 6A). Further, targeting both miRs using respective inhibitors reversed the inhibitory effects of PDGF-BB on RECK expression (Fig. 6A). Since miRs

generally regulate gene expression by binding to the 3' untranslated region (UTR) of target gene mRNA, we next investigated whether miR-221 and miR-222 suppress RECK expression by binding to its 3'-UTR. Our data show that while PDGF-BB suppressed RECK 3'-UTR dependent reporter gene activation (Fig. 6B), mutating miR-221/222 binding site reversed its inhibitory effects (Fig. 6B). These data indicate that miR-221 and miR-222 are essential mediators of PDGF-BB-dependent signaling pathways downstream of NF-κB and AP-1 in suppressing RECK expression (Fig. 6).

3.5. Minocycline inhibits SMC migration and proliferation via RECK induction

We have demonstrated that minocycline inhibits PDGF-BB-induced SMC migration and proliferation (Fig. 1). Since PDGF-BB suppresses RECK expression (Fig. 6), and minocycline is known to enhance *RECK* promoter activity [19], we next determined whether targeting RECK reverses the inhibitory effects of minocycline on PDGF-BB-mediated SMC migration and proliferation. Indeed, minocycline upregulated RECK expression in a dose-dependent manner up to 50 μM (Fig. 7A), however, at a higher dose of 100 μM, RECK expression was lowered, possibly due to reduced cell survival as evidenced by an increase in active (cleaved) caspase-3 levels (Fig. 7B). Further, minocycline (10 μM) upregulated RECK expression in a time-dependent manner, reaching a plateau after 2 hours (Fig. 7C). To further confirm the role of RECK in minocycline's anti-migratory and anti-mitogenic effects, we targeted RECK expression by a lentiviral shRNA (knockdown of RECK is shown as an inset in Fig. 7D, with TIMP3 serving as a off-target). Minocycline suppressed PDGF-BB-induced SMC migration by 80% (Fig. 5D) and proliferation by 50% (Fig. 5E), and these effects were reversed by RECK silencing (Fig.

7D and 7E). These results indicate that RECK is an essential mediator of minocycline-mediated inhibition of PDGF-BB-induced SMC migration and proliferation (Fig. 7).

3.6. RECK overexpression blunts PDGF-BB-induced SMC migration

MMPs play a critical role in extracellular matrix (ECM) degradation and agonist-induced cell migration and proliferation [32]. Since PDGF-BB suppressed RECK (Fig. 6A), and as RECK is a MMP regulator, including MMPs 2 and 9 [9, 17], we hypothesized that forced expression of RECK will attenuate PDGF-BB-induced MMP activation and SMC migration and proliferation. Indeed, PDGF-BB induced activation of both MMPs 2 and 9 (Fig. 8A), an effect markedly inhibited by the pan-MMP inhibitor GM6001, corresponding specific inhibitors (MMP2i and MMP9i), and most importantly, minocycline (Fig. 8A). Furthermore, forced expression of RECK by adenoviral transduction inhibited PDGF-BB-induced MMP2 and MMP9 activation (Fig. 8B). Finally, silencing MMP2 and MMP9, each suppressed PDGF-BB-induced SMC migration (Fig. 8C). Together, these data indicate that increased RECK suppresses PDGF-BB-mediated SMC migration by inhibiting MMP activation (Fig. 8).

4. Discussion

The molecular mechanisms underlying growth factor-induced smooth muscle cell migration and proliferation have yet to be fully investigated. Here we report for the first time that minocycline, a tetracycline antibiotic, inhibits PDGF-BB-mediated human aortic smooth muscle cell (SMC) migration and proliferation by reversing RECK suppression. RECK is an MMP inhibitor, and PDGF-BB suppressed its expression via AKT and ERK activation, ROS generation, NF-κB and AP-1 activation, and miR-221 and miR-222 induction. Notably, RECK overexpression blunted PDGF-BB-mediated MMP activation and SMC migration and proliferation (Fig. 9). These results indicate that minocycline and other RECK inducers have the potential to inhibit vascular proliferative diseases.

Our data show that minocycline inhibited multiple signal transduction pathways activated by PDGF-BB, including AKT, ERK and oxidative stress. In fact, PDGF-BB signals via both PDGFR α and β homo- or heterodimers, and that both receptor subunits have intrinsic tyrosine kinase activity. It has been previously shown that binding of PDGF-BB to PDGFRβ results in receptor tyrosine phosphorylation, and recruitment and activation of various second messengers, including PI3K, resulting in AKT activation, ROS generation, and MAPK activation. PDGF-BB/PDGFRβ signaling has also been shown to induce Ras-dependent ERK activation. Activation of AKT, oxidative stress and ERK all have been shown to contribute to PDGF-BB-mediated cell migration and proliferation. Importantly, our data show that by targeting all three pathways, minocycline inhibited PDGF-BB-mediated SMC migration and proliferation.

Our results also show that minocycline inhibits PDGF-BB-induced superoxide and hydrogen peroxide generation, confirming its antioxidant effects. Minocycline has been shown to inhibit inducible nitric oxide synthase (iNOS) expression and iNOS-dependent nitric oxide

generation. In fact, it has been shown to directly scavenge peroxynitrite, a product of reactive oxygen and reactive nitrogen species. Lipid peroxidation resulting from increased oxidative stress serves as a potential biomarker in vivo, and minocycline has been shown to inhibit lipid peroxidation [33]. By inhibiting inflammatory mediators, minocycline has also been shown to attenuate oxidative stress, suggesting that minocycline targeted multiple pro-oxidant mechanisms. It has been demonstrated that its antioxidant effects stem from the phenol ring structure [34]. In addition to radical scavenging, minocycline has also been shown to attenuate oxidative stress indirectly by enhancing cellular antioxidant systems, such as increasing endogenous levels of glutathione (GSH), and the induction of superoxide dismutase and glutathione peroxidase [35]. Of note, its free radical scavenging effects have been shown to be as effective as vitamin E [34].

In addition to inhibiting ROS generation, our data show that minocycline also inhibited activation of the redox-sensitive transcription factors NF-κB- and AP-1, and miR-221 and miR-222 induction. Moreover, inhibitors of these miRs attenuated PDGF-BB-induced SMC migration and proliferation. The role of NF-κB and AP-1 in miR-221 and miR-222 expression has been previously reported in prostate carcinoma and glioblastoma cells [36]. mir-221 and its paralogue miR-222 are encoded in tandem on the X chromosome and are highly conserved throughout vertebrate animals, including human, rat, and mouse. Their functions have been extensively studied in tumorigenesis and metastasis [37-39]. They are also implicated in cardiovascular diseases [40-42]. For example, in a rat model of injury-induced arterial stenosis, miR-221/222 are shown upregulated in SMCs in neointima and tunica media underneath the lesion [30], and silencing miR-221/222 reduced neointimal thickening [30]. It has been previously reported that PDGF-BB-induced miR-221 targets p27 (Kip1) and c-Kit in cultured vascular SMCs and promotes cell cycle progression and de-differentiation [31]. Here, we found that both miRs -221

and -222 directly target and downregulate RECK expression in SMC, facilitating PDGF-BB-induced proliferation and migration. Interestingly, in addition to targeting RECK, an MMP inhibitor, both miRs have also been shown to target TIMP3 [43], another MMP inhibitor, suggesting that increased expression of both miRs contribute to vascular proliferative diseases by targeting MMP inhibitors. Though we have not investigated, it is highly likely that minocycline might inhibit miR induction by targeting oxidative stress and induction of inflammatory mediators.

Our data also show that minocycline inhibited PDGF-BB-mediated MMP activation. It inhibited activation of both MMPs 2 and 9 in SMC. Multiple mechanisms might have contributed to its inhibitory effects. For example, by targeting oxidative stress and activation of redox-sensitive transcription factors like NF-κB and AP-1, minocycline might have inhibited MMP2 and MMP9 activation. It is also possible that by suppressing the expression of inflammatory mediators, which are known to increase MMP expression and activation. MMPs are zinc-dependent endopeptidases, and minocycline has been shown to chelate Zn2+ [44]. Our data show that minocycline upregulates the expression of RECK, an MMP inhibitor, indicating that minocycline exerts multiple vasculoprotective effects

As discussed earlier, minocycline is a US FDA-approved broad-spectrum tetracycline antibiotic. It has been on the market for more than 40 years and is prescribed as an oral or systemic medication for treating acne vulgaris, skin infections, and sexually transmitted diseases. Its short and relatively long term (~ 2 years) effects have also been tested as an-arthritic drug in human subjects [45-49], with positive results. Such a history of safe use in human subjects even in a relatively longterm application provides further support of minocycline's therapeutic potential in cardiovascular diseases. However, some limitations have been identified. Even

though considered rare, minocycline administration has been shown to induce liver damage in some subjects [50, 51]. Similarly, in a rat model of restenosis, minocycline administration inhibited neointimal hyperplasia following arterial injury, but induced liver toxicity at the therapeutic dose [7]. On the other hand, in a mouse model of atherosclerosis, minocycline effectively prevented atherosclerosis and did not induce liver damage [8]. These reports suggest that the range of the effective dose of minocycline may be narrow in human vascular proliferative diseases, and thus should be carefully evaluated. Also in general, the long-term use of antibiotics will result in antimicrobial resistance. Chemical engineering that mitigates the antibacterial activity and toxicity may improve minocycline's potential as an effective therapeutic in vascular proliferative diseases. Alternatively, it would be useful to identify a downstream effector of minocycline as a novel therapeutic agent, such as RECK induction. In summary, our results suggest that the induction of RECK is one of the mechanisms by which minocycline exerts vasculoprotective effects. Our results also suggest that RECK inducers may have the potential to inhibit vascular proliferative diseases.

Conflicts of interest

The authors declare no conflict of interest.

Acknowledgments

BC is a recipient of the Department of Veterans Affairs *Research Career Scientist* award (#IK6BX004016-01), and is supported by the U.S. Department of Veterans Affairs, Office of Research and Development-Biomedical Laboratory Research and Development (ORD-BLRD) Service Award VA-I01-BX002255. Work in SM's lab is supported by NIH/NIAID R01AI119131. SS is supported by NIH R21-HL113705, PD by HL080682 and 1-U54 GM104940, and TY by American Heart Association 15SDG25240022.

Abbreviations

Ad.siMMP, Adenoviral vector expressing MMP2 siRNA; AKT, V-Akt Murine Thymoma Viral Oncogene; AP-1, Activator Protein-1; ERK, Extracellular Signal Regulated Kinase; GFP, Green Fluorescent Protein; eGFP, enhanced GFP; SMC, smooth muscle cells; IKKβ, Inhibitor of Nuclear Factor Kappa B Kinase Subunit Beta; JNK, c-Jun N-terminal kinase; MAP, Mitogen Activated Protein kinase; miR, micro RNA; MMP, matrix metallopeptidase; moi, multiplicity of infection; MTT, 3-(4,5-dimethylthiazol-2-yl)-2,5-diphenyltetrazolium bromide; NAC, N-acetyl-L-Cysteine; NF-κB, Nuclear Factor κB; Nox, NADPH oxidase; NADPH, Nicotinamide adenine dinucleotide phosphate; PDGF, platelet-derived growth factor; PET, polyethylene terephthalate;; PI3K, Phosphoinositide-3-kinase; PARP-1, Poly(ADP-Ribose) Polymerase; RECK, Reversion Inducing Cysteine Rich Protein with Kazal Motifs; shRNA, short hairpin RNA; siRNA, small interference RNA; UTR, untranslated region; VEGF, Vascular Endothelial Growth Factor.

References

[1] A. Jawien, D.F. Bowen-Pope, V. Lindner, S.M. Schwartz, A.W. Clowes, Platelet-derived growth factor promotes smooth muscle migration and intimal thickening in a rat model of balloon angioplasty, J Clin Invest 89(2) (1992) 507-11.
[2] G.A. Ferns, E.W. Raines, K.H. Sprugel, A.S. Motani, M.A. Reidy, R. Ross, Inhibition of neointimal smooth muscle accumulation after angioplasty by an antibody to PDGF, Science 253(5024) (1991) 1129-32.
[3] P.H. Chen, X. Chen, X. He, Platelet-derived growth factors and their receptors: structural and functional perspectives, Biochim Biophys Acta 1834(10) (2013) 2176-86.
[4] L.M. Graves, K.E. Bornfeldt, E.W. Raines, B.C. Potts, S.G. Macdonald, R. Ross, E.G. Krebs, Protein kinase A antagonizes platelet-derived growth factor-induced signaling by mitogen-activated protein kinase in human arterial smooth muscle cells, Proc Natl Acad Sci U S A 90(21) (1993) 10300-4.
[5] Z. Yang, B.S. Oemar, T. Carrel, B. Kipfer, F. Julmy, T.F. Luscher, Different proliferative properties of smooth muscle cells of human arterial and venous bypass vessels: role of PDGF receptors, mitogen-activated protein kinase, and cyclin-dependent kinase inhibitors, Circulation 97(2) (1998) 181-7.
[6] J.S. Yao, Y. Chen, W. Zhai, K. Xu, W.L. Young, G.Y. Yang, Minocycline exerts multiple inhibitory effects on vascular endothelial growth factor-induced smooth muscle cell migration: the role of ERK1/2, PI3K, and matrix metalloproteinases, Circ Res 95(4) (2004) 364-71.
[7] S.P. Pinney, H.J. Chen, D. Liang, X. Wang, A. Schwartz, L.E. Rabbani, Minocycline inhibits smooth muscle cell proliferation, migration and neointima formation after arterial injury, J Cardiovasc Pharmacol 42(4) (2003) 469-76.
[8] K. Shahzad, M. Thati, H. Wang, M. Kashif, J. Wolter, S. Ranjan, T. He, Q. Zhou, E. Blessing, A. Bierhaus, P.P. Nawroth, B. Isermann, Minocycline reduces plaque size in diet induced atherosclerosis via p27(Kip1), Atherosclerosis 219(1) (2011) 74-83.
[9] J. Oh, R. Takahashi, S. Kondo, A. Mizoguchi, E. Adachi, R.M. Sasahara, S. Nishimura, Y. Imamura, H. Kitayama, D.B. Alexander, C. Ide, T.P. Horan, T. Arakawa, H. Yoshida, S. Nishikawa, Y. Itoh, M. Seiki, S. Itohara, C. Takahashi, M. Noda, The membrane-anchored MMP inhibitor RECK is a key regulator of extracellular matrix integrity and angiogenesis, Cell 107(6) (2001) 789-800.
[10] M. Noda, H. Kitayama, T. Matsuzaki, Y. Sugimoto, H. Okayama, R.H. Bassin, Y. Ikawa, Detection of genes with a potential for suppressing the transformed phenotype associated with activated ras genes, Proc Natl Acad Sci U S A 86(1) (1989) 162-6.
[11] H. Kitayama, Y. Sugimoto, T. Matsuzaki, Y. Ikawa, M. Noda, A ras-related gene with transformation suppressor activity, Cell 56(1) (1989) 77-84.
[12] C. Takahashi, N. Akiyama, T. Matsuzaki, S. Takai, H. Kitayama, M. Noda, Characterization of a human MSX-2 cDNA and its fragment isolated as a transformation suppressor gene against v-Ki-ras oncogene, Oncogene 12(10) (1996) 2137-46.
[13] A.I. Su, T. Wiltshire, S. Batalov, H. Lapp, K.A. Ching, D. Block, J. Zhang, R. Soden, M. Hayakawa, G. Kreiman, M.P. Cooke, J.R. Walker, J.B. Hogenesch, A gene atlas of the mouse and human protein-encoding transcriptomes, Proc Natl Acad Sci U S A 101(16) (2004) 6062-7.
[14] Y. Yoshida, K. Ninomiya, H. Hamada, M. Noda, Involvement of the SKP2-p27(KIP1) pathway in suppression of cancer cell proliferation by RECK, Oncogene 31(37) (2012) 4128-38.

[15] J.M. Siddesha, A.J. Valente, S.S. Sakamuri, T. Yoshida, J.D. Gardner, N. Somanna, C. Takahashi, M. Noda, B. Chandrasekar, Angiotensin II stimulates cardiac fibroblast migration via the differential regulation of matrixins and RECK, J Mol Cell Cardiol 65 (2013) 9-18.
[16] J.M. Siddesha, A.J. Valente, T. Yoshida, S.S. Sakamuri, P. Delafontaine, H. Iba, M. Noda, B. Chandrasekar, Docosahexaenoic acid reverses angiotensin II-induced RECK suppression and cardiac fibroblast migration, Cell Signal 26(5) (2014) 933-41.
[17] C. Takahashi, Z. Sheng, T.P. Horan, H. Kitayama, M. Maki, K. Hitomi, Y. Kitaura, S. Takai, R.M. Sasahara, A. Horimoto, Y. Ikawa, B.J. Ratzkin, T. Arakawa, M. Noda, Regulation of matrix metalloproteinase-9 and inhibition of tumor invasion by the membrane-anchored glycoprotein RECK, Proc Natl Acad Sci U S A 95(22) (1998) 13221-6.
[18] M. Noda, J. Oh, R. Takahashi, S. Kondo, H. Kitayama, C. Takahashi, RECK: a novel suppressor of malignancy linking oncogenic signaling to extracellular matrix remodeling, Cancer Metastasis Rev 22(2-3) (2003) 167-75.
[19] R. Murai, Y. Yoshida, T. Muraguchi, E. Nishimoto, Y. Morioka, H. Kitayama, S. Kondoh, Y. Kawazoe, M. Hiraoka, M. Uesugi, M. Noda, A novel screen using the Reck tumor suppressor gene promoter detects both conventional and metastasis-suppressing anticancer drugs, Oncotarget 1(4) (2010) 252-64.
[20] F.E. Rey, M.E. Cifuentes, A. Kiarash, M.T. Quinn, P.J. Pagano, Novel competitive inhibitor of NAD(P)H oxidase assembly attenuates vascular O(2)(-) and systolic blood pressure in mice, Circ Res 89(5) (2001) 408-14.
[21] B. Venkatesan, A.J. Valente, V.S. Reddy, D.A. Siwik, B. Chandrasekar, Resveratrol blocks interleukin-18-EMMPRIN cross-regulation and smooth muscle cell migration, Am J Physiol Heart Circ Physiol 297(2) (2009) H874-86.
[22] B. Venkatesan, A.J. Valente, N.A. Das, A.J. Carpenter, T. Yoshida, J.L. Delafontaine, U. Siebenlist, B. Chandrasekar, CIKS (Act1 or TRAF3IP2) mediates high glucose-induced endothelial dysfunction, Cell Signal 25(1) (2013) 359-71.
[23] J. Padilla, A.J. Carpenter, N.A. Das, H.K. Kandikattu, S. Lopez-Ongil, L.A. Martinez-Lemus, U. Siebenlist, V.G. DeMarco, B. Chandrasekar, TRAF3IP2 mediates high glucose-induced endothelin-1 production as well as endothelin-1-induced inflammation in endothelial cells, Am J Physiol Heart Circ Physiol 314(1) (2018) H52-H64.
[24] A.J. Valente, A.M. Irimpen, U. Siebenlist, B. Chandrasekar, OxLDL induces endothelial dysfunction and death via TRAF3IP2: inhibition by HDL3 and AMPK activators, Free Radic Biol Med 70 (2014) 117-28.
[25] A.J. Valente, R.A. Clark, J.M. Siddesha, U. Siebenlist, B. Chandrasekar, CIKS (Act1 or TRAF3IP2) mediates Angiotensin-II-induced Interleukin-18 expression, and Nox2-dependent cardiomyocyte hypertrophy, J Mol Cell Cardiol 53(1) (2012) 113-24.
[26] W. Liu, N. Song, H. Yao, L. Zhao, H. Liu, G. Li, miR-221 and miR-222 Simultaneously Target RECK and Regulate Growth and Invasion of Gastric Cancer Cells, Med Sci Monit 21 (2015) 2718-25.
[27] N.K. Somanna, M. Yariswamy, J.M. Garagliano, U. Siebenlist, S. Mummidi, A.J. Valente, B. Chandrasekar, Aldosterone-induced cardiomyocyte growth, and fibroblast migration and proliferation are mediated by TRAF3IP2, Cell Signal 27(10) (2015) 1928-38.
[28] J.A. Romashkova, S.S. Makarov, NF-kappaB is a target of AKT in anti-apoptotic PDGF signalling, Nature 401(6748) (1999) 86-90.

[29] Y. Zhan, S. Kim, H. Yasumoto, M. Namba, H. Miyazaki, H. Iwao, Effects of dominant-negative c-Jun on platelet-derived growth factor-induced vascular smooth muscle cell proliferation, Arterioscler Thromb Vasc Biol 22(1) (2002) 82-8.
[30] X. Liu, Y. Cheng, S. Zhang, Y. Lin, J. Yang, C. Zhang, A necessary role of miR-221 and miR-222 in vascular smooth muscle cell proliferation and neointimal hyperplasia, Circ Res 104(4) (2009) 476-87.
[31] B.N. Davis, A.C. Hilyard, P.H. Nguyen, G. Lagna, A. Hata, Induction of microRNA-221 by platelet-derived growth factor signaling is critical for modulation of vascular smooth muscle phenotype, J Biol Chem 284(6) (2009) 3728-38.
[32] A.C. Newby, Matrix metalloproteinases regulate migration, proliferation, and death of vascular smooth muscle cells by degrading matrix and non-matrix substrates, Cardiovasc Res 69(3) (2006) 614-24.
[33] E. Sonmez, S. Kabatas, O. Ozen, G. Karabay, S. Turkoglu, E. Ogus, C. Yilmaz, H. Caner, N. Altinors, Minocycline treatment inhibits lipid peroxidation, preserves spinal cord ultrastructure, and improves functional outcome after traumatic spinal cord injury in the rat, Spine (Phila Pa 1976) 38(15) (2013) 1253-9.
[34] R.L. Kraus, R. Pasieczny, K. Lariosa-Willingham, M.S. Turner, A. Jiang, J.W. Trauger, Antioxidant properties of minocycline: neuroprotection in an oxidative stress assay and direct radical-scavenging activity, J Neurochem 94(3) (2005) 819-27.
[35] K. Shahzad, F. Bock, M.M. Al-Dabet, I. Gadi, S. Nazir, H. Wang, S. Kohli, S. Ranjan, P.R. Mertens, P.P. Nawroth, B. Isermann, Stabilization of endogenous Nrf2 by minocycline protects against Nlrp3-inflammasome induced diabetic nephropathy, Sci Rep 6 (2016) 34228.
[36] S. Galardi, N. Mercatelli, M.G. Farace, S.A. Ciafre, NF-kB and c-Jun induce the expression of the oncogenic miR-221 and miR-222 in prostate carcinoma and glioblastoma cells, Nucleic Acids Res 39(9) (2011) 3892-902.
[37] M. Garofalo, C. Quintavalle, G. Romano, C.M. Croce, G. Condorelli, miR221/222 in cancer: their role in tumor progression and response to therapy, Curr Mol Med 12(1) (2012) 27-33.
[38] M.Y. Shah, G.A. Calin, MicroRNAs miR-221 and miR-222: a new level of regulation in aggressive breast cancer, Genome Med 3(8) (2011) 56.
[39] W. Lou, J. Liu, Y. Gao, G. Zhong, D. Chen, J. Shen, C. Bao, L. Xu, J. Pan, J. Cheng, B. Ding, W. Fan, MicroRNAs in cancer metastasis and angiogenesis, Oncotarget 8(70) (2017) 115787-115802.
[40] T. Celic, V. Metzinger-Le Meuth, I. Six, Z.A. Massy, L. Metzinger, The mir-221/222 Cluster is a Key Player in Vascular Biology via the Fine-Tuning of Endothelial Cell Physiology, Curr Vasc Pharmacol 15(1) (2017) 40-46.
[41] Y. Wei, A. Schober, C. Weber, Pathogenic arterial remodeling: the good and bad of microRNAs, Am J Physiol Heart Circ Physiol 304(8) (2013) H1050-9.
[42] S. Albinsson, W.C. Sessa, Can microRNAs control vascular smooth muscle phenotypic modulation and the response to injury?, Physiol Genomics 43(10) (2011) 529-33.
[43] M. Garofalo, G. Di Leva, G. Romano, G. Nuovo, S.S. Suh, A. Ngankeu, C. Taccioli, F. Pichiorri, H. Alder, P. Secchiero, P. Gasparini, A. Gonelli, S. Costinean, M. Acunzo, G. Condorelli, C.M. Croce, miR-221&222 regulate TRAIL resistance and enhance tumorigenicity through PTEN and TIMP3 downregulation, Cancer Cell 16(6) (2009) 498-509.
[44] L. Lambs, M. Brion, G. Berthon, Metal ion-tetracycline interactions in biological fluids. Part 3. Formation of mixed-metal ternary complexes of tetracycline, oxytetracycline,

doxycycline and minocycline with calcium and magnesium, and their involvement in the bioavailability of these antibiotics in blood plasma, Agents Actions 14(5-6) (1984) 743-50.
[45] M. Kloppenburg, F.C. Breedveld, J.P. Terwiel, C. Mallee, B.A. Dijkmans, Minocycline in active rheumatoid arthritis. A double-blind, placebo-controlled trial, Arthritis Rheum 37(5) (1994) 629-36.
[46] J.R. O'Dell, C.E. Haire, W. Palmer, W. Drymalski, S. Wees, K. Blakely, M. Churchill, P.J. Eckhoff, A. Weaver, D. Doud, N. Erikson, F. Dietz, R. Olson, P. Maloley, L.W. Klassen, G.F. Moore, Treatment of early rheumatoid arthritis with minocycline or placebo: results of a randomized, double-blind, placebo-controlled trial, Arthritis Rheum 40(5) (1997) 842-8.
[47] J.R. O'Dell, K.W. Blakely, J.A. Mallek, P.J. Eckhoff, R.D. Leff, S.J. Wees, K.M. Sems, A.M. Fernandez, W.R. Palmer, L.W. Klassen, G.A. Paulsen, C.E. Haire, G.F. Moore, Treatment of early seropositive rheumatoid arthritis: a two-year, double-blind comparison of minocycline and hydroxychloroquine, Arthritis Rheum 44(10) (2001) 2235-41.
[48] M. Stone, P.R. Fortin, C. Pacheco-Tena, R.D. Inman, Should tetracycline treatment be used more extensively for rheumatoid arthritis? Metaanalysis demonstrates clinical benefit with reduction in disease activity, J Rheumatol 30(10) (2003) 2112-22.
[49] B.C. Tilley, G.S. Alarcon, S.P. Heyse, D.E. Trentham, R. Neuner, D.A. Kaplan, D.O. Clegg, J.C. Leisen, L. Buckley, S.M. Cooper, H. Duncan, S.R. Pillemer, M. Tuttleman, S.E. Fowler, Minocycline in rheumatoid arthritis. A 48-week, double-blind, placebo-controlled trial. MIRA Trial Group, Ann Intern Med 122(2) (1995) 81-9.
[50] T.J. Urban, P. Nicoletti, N. Chalasani, J. Serrano, A. Stolz, A.K. Daly, G.P. Aithal, J. Dillon, V. Navarro, J. Odin, H. Barnhart, D. Ostrov, N. Long, E.T. Cirulli, P.B. Watkins, R.J. Fontana, N. Drug-Induced Liver Injury, g. Pharmacogenetics of Drug-Induced Liver Injury, C. International Serious Adverse Events, Minocycline hepatotoxicity: Clinical characterization and identification of HLA-B *35:02 as a risk factor, J Hepatol 67(1) (2017) 137-144.
[51] R.A. Lawrenson, H.E. Seaman, A. Sundstrom, T.J. Williams, R.D. Farmer, Liver damage associated with minocycline use in acne: a systematic review of the published literature and pharmacovigilance data, Drug Saf 23(4) (2000) 333-49.

Figure legends

Figure 1. **Minocycline inhibits PDGF-BB-mediated AKT-dependent SMC migration and proliferation**. A, PDGF-BB induces time-dependent AKT activation. At 70-80% confluency, SMC were made quiescent by incubating for 48 h in Ham's-F12/0.5% BSA, treated with PDGF-BB (=10 ng/ml) for the indicated time period. AKT activation was analyzed in cleared whole cell lysates using antibodies that detect activation-specific antibodies. Total AKT served as a control (n=3). B, Minocycline inhibits PDGF-BB-induced PI3K-dependent AKT activation. Quiescent SMC were incubated with the PI3K inhibitor Wortmannin (100 nM in DMSO for 1h), the AKT inhibitor MK2206 (5μM for 1h), or minocycline (10 μM for 15 min) prior to PDGF-BB addition (10 ng/ml for 30 min). AKT activation was analyzed as in A (n=3). C, Minocycline inhibits PI3K/AKT-dependent SMC migration. Quiescent SMC were layered on Matrigel™ basement membrane matrix-coated filters, incubated with Wortmannin, MK2206 or minocycline as in B prior to PDGF-BB (10 ng/ml) addition. The lower chamber contained 20% FBS. After 18h, cells migrated to the lower side of the membrane were quantified using MTT assay (n=6). D, Minocycline inhibits PI3K/AKT-dependent SMC proliferation without modulating cell viability. Quiescent SMC incubated as in B were analyzed for proliferation after 48h by CyQUANT® Cell Proliferation Assay (n=8). Activation of caspase-3, as an indication of reduced cell viability, was analyzed by immnoblotting (inset, n=3). Hydrogen peroxide (H_2O_2, 100 μM) served as a positive control. A, B, Immunoreactive bands from three independent experiments were semiquantified by densotometry, and summarized in the respective lower panels. *P< 0.01 vs. untreated, †P< at least 0.05 vs. PDGF-BB (n=6).

Figure 2. **Minocycline inhibits PDGF-BB-mediated ERK-dependent SMC migration and proliferation**. A, PDGF-BB induces time-dependent ERK activation. At 70-80% confluency, SMC were made quiescent by incubating for 48 h in Ham's-F12/0.5% BSA, treated with PDGF-BB (=10 ng/ml) for the indicated time period. ERK activation was analyzed in cleared whole cell lysates using antibodies that detect activation-specific antibodies. Total ERK served as a control (n=3). B, Minocycline inhibits PDGF-BB-induced ERK activation. Quiescent SMC were incubated with the ERK inhibitor SCH772984 (10μM in DMSO for 1 h) or minocycline (10 μM for 15 min) prior to PDGF-BB addition (10 ng/ml for 30 min). ERK activation was analyzed as in A (n=3). C, Minocycline inhibits ERK-dependent SMC migration. Quiescent SMC were layered on Matrigel™ basement membrane matrix-coated filters, incubated with SCH772984 or minocycline as in B prior to PDGF-BB (10 ng/ml) addition. The lower chamber contained 20% FBS. After 18h, cells migrated to the lower side of the membrane were quantified using MTT assay (n=6). D, Minocycline inhibits ERK-dependent SMC proliferation without modulating cell viability. Quiescent SMC incubated as in B were analyzed for proliferation after 48h by CyQUANT® Cell Proliferation Assay (n=8). Activation of caspase-3, as an indication of reduced cell viability, was analyzed by immnoblotting (inset, n=3). Hydrogen peroxide (H_2O_2, 100 μM) served as a positive control. A, B, Immunoreactive bands from three independent experiments were semiquantified by densotometry, and summarized in the respective lower panels. *P< 0.01 vs. untreated, †P< at least 0.05 vs. PDGF-BB (n=6).

Figure 3. Minocycline inhibits PDGF-BB-induced oxidative stress and oxidative stress-responsive SMC migration and proliferation. A, B, Minocycline inhibits PDGF-BB-induced superoxide and hydrogen peroxide (H_2O_2) generation. Quiescent SMC were incubated

with PDGF-BB for 15 (A) or 30 (B) min. Superoxide anion ($O_2^{-\bullet}$; A) and H_2O_2 (B) production were analyzed by cytochrome C assay and Amplex red assay, respectively (n=6). In a subset of experiments, quiescent SMC were incubated with NAC (5mM in water for 30 min), a peptide inhibitor of Nox2 (gp91 ds-tat; 1 μM for 1 h), the Nox1/4 inhibitor GKT137831 (5 μM in DMSO for 15 min) or minocycline (10 μM for 15 min) prior to PDGF-BB addition. Scrambled gp91 ds-tat (sgp91 ds-tat) and DMSO served as controls. C, Minocycline inhibits PDGF-BB-induced oxidative stress-responsive SMC migration. Quiescent SMC were layered on Matrigel™ basement membrane matrix-coated filters, incubated with PDGF-BB (10 ng/ml) for 18 h. The lower chamber contained 20% FBS. Cells migrated to the lower side of the membrane were quantified using MTT assay. In a subset of experiments, SMC were treated with NAC, gp91 ds-tat, GKT137831, or minocycline as A and B prior to PDGF-BB addition. D, E, Minocycline inhibits PDGF-BB-induced SMC proliferation (D) without affecting cell viability (E). Quiescent SMC incubated as in A and B were analyzed for proliferation after 48h by CyQUANT® Cell Proliferation Assay. Activation of caspase-3, as an indication of reduced cell viability, was analyzed by immnoblotting (E, n=3). Hydrogen peroxide (H_2O_2, 100 μM) served as a positive control. *P< 0.01 vs. untreated, †P< 0.01 vs. PDGF-BB (n=6).

Figure 4. **Minocycline inhibits PDGF-BB-induced NF-κB and AP-1 activation.** A, PDGF-BB induces time-dependent NF-κB activation. Quiescent SMC were incubated with PDGF-BB (10 ng/ml). At the indicated time periods, activation of NF-κB was analyzed by immunoblotting using antibodies that specifically detect phosphorylated p65 at Ser^{536}. B, PDGF-BB induces time-dependent AP-1 activation. Quiescent SMC incubated as in A were analyzed for AP-1 activation by immunoblotting using antibodies that specifically detect phosphorylated

c-Jun at Ser[73]. C, Silencing IKKβ or pre-treatment with minocycline inhibit PDGF-BB-induced NF-κB activation. SMC incubated with lentiviral IKKβ shRNA (moi0.5 for 48 h) were made quiescent and treated with PDGF-BB (10 ng/ml for 30 min). In a subset of experiments, quiescent SMC were incubated with minocycline (10 μM for 15 min) and then treated with PDGF-BB (10 ng/ml for 30 min). Activation of NF-κB was analyzed as in *A*. D, Silencing JNK2 or pre-treatment with minocycline inhibits PDGF-BB-induced AP-1 activation. SMC incubated with lentiviral JNK2 shRNA (moi 0.5 for 48 h) were made quiescent and treated with PDGF-BB (10 ng/ml for 30 min). In a subset of experiments, quiescent SMC were incubated with minocycline (10 mM for 15 min) and then treated with PDGF-BB (10 ng/ml for 30 min). Activation of AP-1 was analyzed as in *B*. Silencing IKKβ and JNK2 was confirmed by immunoblotting. JNK2 and IKKβ served as off-targets in IKKβ and JNK2 silenced cells, respectively (right hand panels in C and D). Tubulin served as a loading control. Bar graphs at the bottom of panels in A-D represent densitometric analyses from three independent experiments. **P*<0.05 control, †*P*<0.05 *versus* PDGF-BB (n=3).

Figure 5. **PDGF-BB induces SMC proliferation in part via miR-221 and miR-222**. A, B, PDGF-BB induces miR-221 (A) and miR-222 (B) expression via IKKβ, NF-κB, JNK and AP-1. Quiescent SMC incubated with PDGF-BB (10 ng/ml) for 1h were analyzed for miR-221 (A) and miR-222 (B) expression by TaqMan® Advanced miRNA assays. The results were normalized to corresponding U6 expression. In a subset of experiments, SMC were incubated with lentiviral IKKβ, p65, JNK2 or c-Jun shRNA (moi0.5 for 48 h), made quiescent and then treated with PDGF-BB addition. C, D, miR-221 and miR-222 mediate PDGF-induced SMC migration (C) and proliferation (D), without affecting cell viability (E). SMC were transduced

with miR-221 or miR-222 inhibitors prior to the addition of PDGF-BB (10 ng/ml). Cell migration was analyzed after 18 h using transwell migration assays (C). Cell proliferation was analyzed after 48h by CyQUANT® Cell Proliferation Assay (D). Cleaved caspase-3 levels, indicative of cells undergoing apoptosis, was analyzed after 8 h by immunoblotting using antibodies that detect both total and cleaved caspase-3 levels (E). Hydrogen peroxide (H_2O_2, 100 μM) served as a positive control. *P<at least 0.05 *versus* control, †P<0.05 *versus* PDGF-BB (n=6).

Figure 6. **PDGF suppresses RECK expression via miR-221 and miR-222**. A, Inhibitors of miR-221 and miR-222 reverse PDGF-BB-induced RECK suppression. Quiescent SMC were transfected with miR-221 or miR-222 inhibitor or the negative control (80 nM) using the Neon® transfection system. Twenty four-hours later, cells were treated with PDGF-BB (10 ng/ml for 24 h), and then analyzed for RECK protein levels by immunoblotting (n=3). B, Mutating miR-221/miR-222 binding site in RECK 3'UTR reverses PDGF-BB-induced RECK suppression. SMC transfected with wild type (WT) or miR-221/222 mutant (mutant) RECK 3'UTR reporter vector (3 μg) along with pRL-Tk vector (100 ng) for 24 h were treated with PDGF-BB (10 ng/ml for 12 h), and then harvested for dual luciferase activity (n=6). *P < at least 0.05 *versus* untreated, †P < at least 0.05 *versus* PDGF-BB (A) or WT (B) mutant RECK 3'UTR (n=3-6).

Figure 7. **Minocycline inhibits PDGF-BB-induced SMC migration and proliferation in part by upregulating RECK expression**. A, Minocycline induces RECK expression in a dose-dependent manner. Quiescent SMC were treated with minocycline at indicated

concentrations for 2h, and analyzed for RECK induction by immunoblotting (n=3). B, Minocycline induces SMC death only at a higher concentration. Quiescent SMC were treated with minocycline at the indicated doses for 12 h, and analyzed for total and cleaved caspase-3 levels by immunoblotting (n=3). C, Minocycline induces RECK expression in a time-dependent manner. Quiescent SMC incubated with minocycline (10 μM) for the indicated time periods were analyzed for RECK expression by immunoblotting as in A (n=3). D, Silencing RECK reverses the inhibitory effects of minocycline on PDGF-BB-induced SMC migration. Quiescent SMC layered on Matrigel™ basement membrane matrix-coated filters were treated with minocycline (10 μM for 15 min) prior to the addition of PDGF-BB (10 ng/ml for 18 h). The lower chamber contained 20% FBS. Cells migrated to the lower side of the membrane were quantified using MTT assay (n=6). E, Silencing RECK reverses the inhibitory effects of minocycline on PDGF-BB-induced SMC proliferation. Quiescent SMC incubated as in D, but for 48 h, and analyzed for proliferation by CyQUANT® Cell Proliferation Assay (n=6). *P<at least 0.05 *versus* control, †P<0.05 *versus* PDGF-BB, §P<0.05 *versus* PDGF-BB+minocycline (n=3-6).

Figure 8. **Minocycline and forced expression of RECK inhibit PDGF-BB-induced MMP-2 and MMP-9 activation**. A, Minocycline inhibits PDGF-BB-induced MMP2 (left panel) and MMP9 (right panel) activation. Quiescent SMC were incubated with minocycline (10 μM for 2 h) prior to PDGF-BB addition (10 ng/ml for 2 h). Activation of MMP2 and MMP9 were analyzed by immunoblotting using antibodies that detect both pro and active forms (n=3). In a subset of experiments, quiescent SMC were incubated with inhibitors of MMP2 (MMP2i-II; 2.5 mM in DMSO for 1 h), MMP9i (100 nM in DMSO for 1 h), or pan-specific MMP inhibitor

GM6001 (10 μM in DMSO for 15 min) prior to PDGF-BB addition. B, Forced expression of RECK inhibits MMP2 and MMP9 activation. SMC were transduced with adenoviral RECK (moi 10 for 24 h) prior to PDGF-BB addition (10 ng/ml for 2 h). Activation of MMP2 (left panel) and MMP9 (right panel) were analyzed as in A (n=3). C, Silencing MMP2 or MMP9 attenuates PDGF-BB-induced SMC migration. SMC transduced with adenoviral MMP2 or MMP9 siRNA (moi100 for 48 h) were treated with PDGF-BB (10 ng/ml for 18 h) and then analyzed for migration (n=6). Knockdown of MMP2 and MMP9 was analyzed by immunoblotting as shown on the right. MMP9 and MMP2 served as off-targets in MMP2 and MMP9 silenced cells, respectively. *P<at least 0.05 *versus* control, †P<0.05 *versus* PDGF-BB (n=3-6).

Figure 9. Schema showing the possible signal transduction pathways targeted by minocycline in reversing PDGF-BB-mediated RECK suppression and human aortic smooth muscle cell proliferation and migration. While PDGF-BB induced AKT and ERK activation, oxidative stress, NF-κB and AP-1 activation, miR-221 and miR-222 induction, MMP activation, and RECK suppression, resulting ultimately in SMC proliferation and migration. Pretreatment with minocycline reversed these effects (blue arrowheads). Moreover, minocycline induced RECK expression (red diamond) and silencing RECK reversed the inhibitory effects of minocycline on PDGF-BB-induced MMP activation and SMC migration and proliferation. These results suggest a therapeutic potential for minocycline in vascular proliferative diseases. Broken arrows: Published reports.

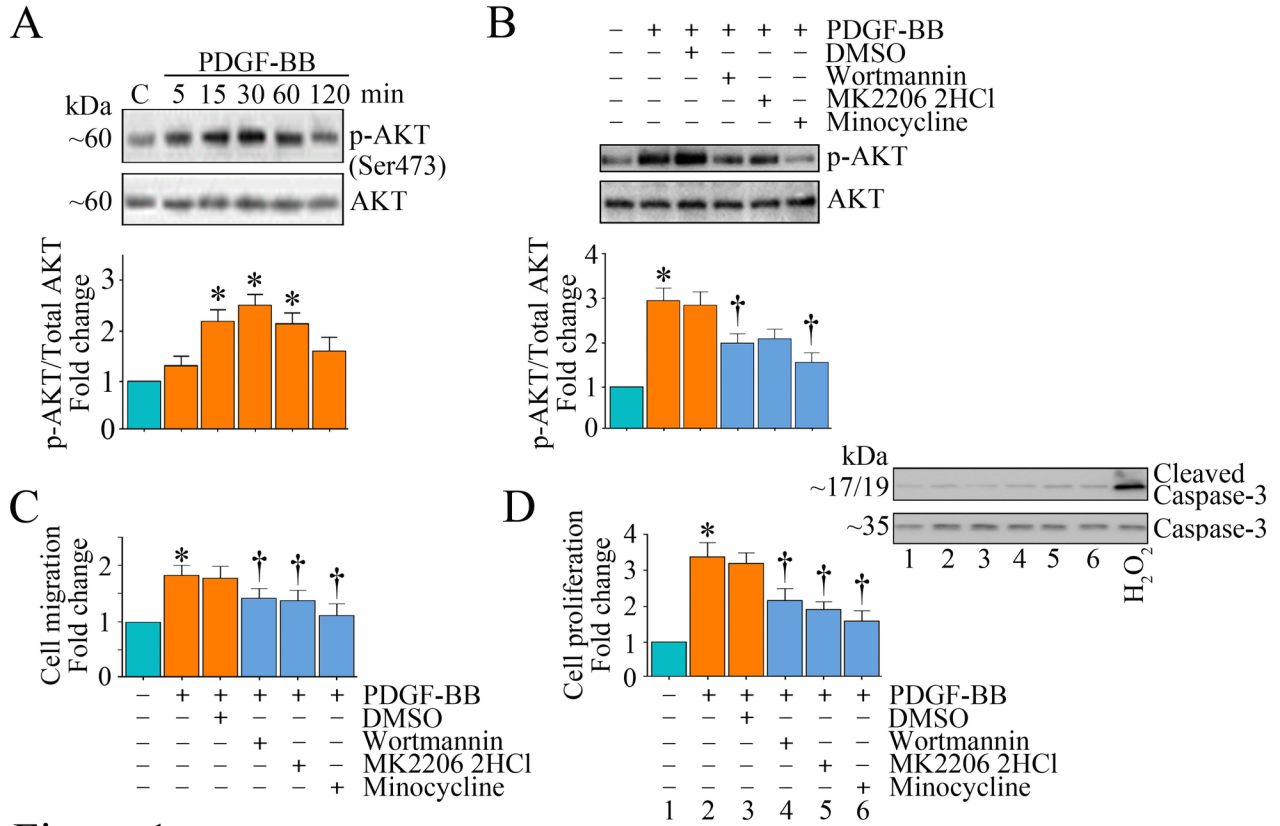
A
PDGF-BB
C 5 15 30 60 120 min
kDa
~60
p-AKT
(Ser473)
~60
AKT
p-AKT/Total AKT
Fold change
B
PDGF-BB
DMSO
Wortmannin
MK2206 2HCl
Minocycline
p-AKT
AKT
p-AKT/Total AKT
Fold change
kDa
~17/19
Cleaved
Caspase-3
~35
Caspase-3
1 2 3 4 5 6
H2O2
C
Cell migration
Fold change
PDGF-BB
DMSO
Wortmannin
MK2206 2HCl
Minocycline
D
Cell proliferation
Fold change
PDGF-BB
DMSO
Wortmannin
MK2206 2HCl
Minocycline
1 2 3 4 5 6

Figure 1

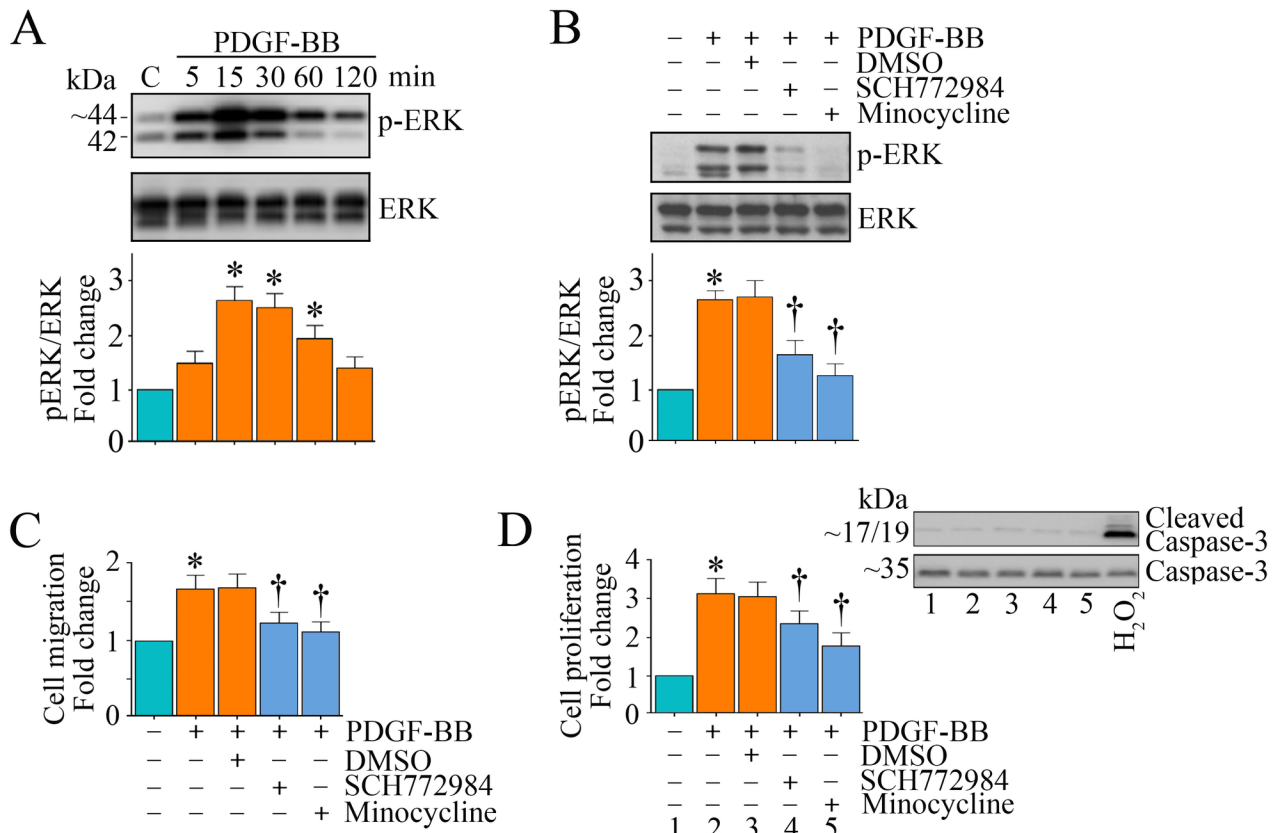
A
PDGF-BB
kDa C 5 15 30 60 120 min
~44
42
p-ERK
ERK
pERK/ERK Fold change
B
– + + + + PDGF-BB
– – + – – DMSO
– – – + – SCH772984
– – – – + Minocycline
p-ERK
ERK
pERK/ERK Fold change
C
Cell migration Fold change
– + + + + PDGF-BB
– – + – – DMSO
– – – + – SCH772984
– – – – + Minocycline
D
Cell proliferation Fold change
kDa
~17/19
Cleaved Caspase-3
~35
Caspase-3
1 2 3 4 5
H2O2
– + + + + PDGF-BB
– – + – – DMSO
– – – + – SCH772984
– – – – + Minocycline
1 2 3 4 5

Figure 2

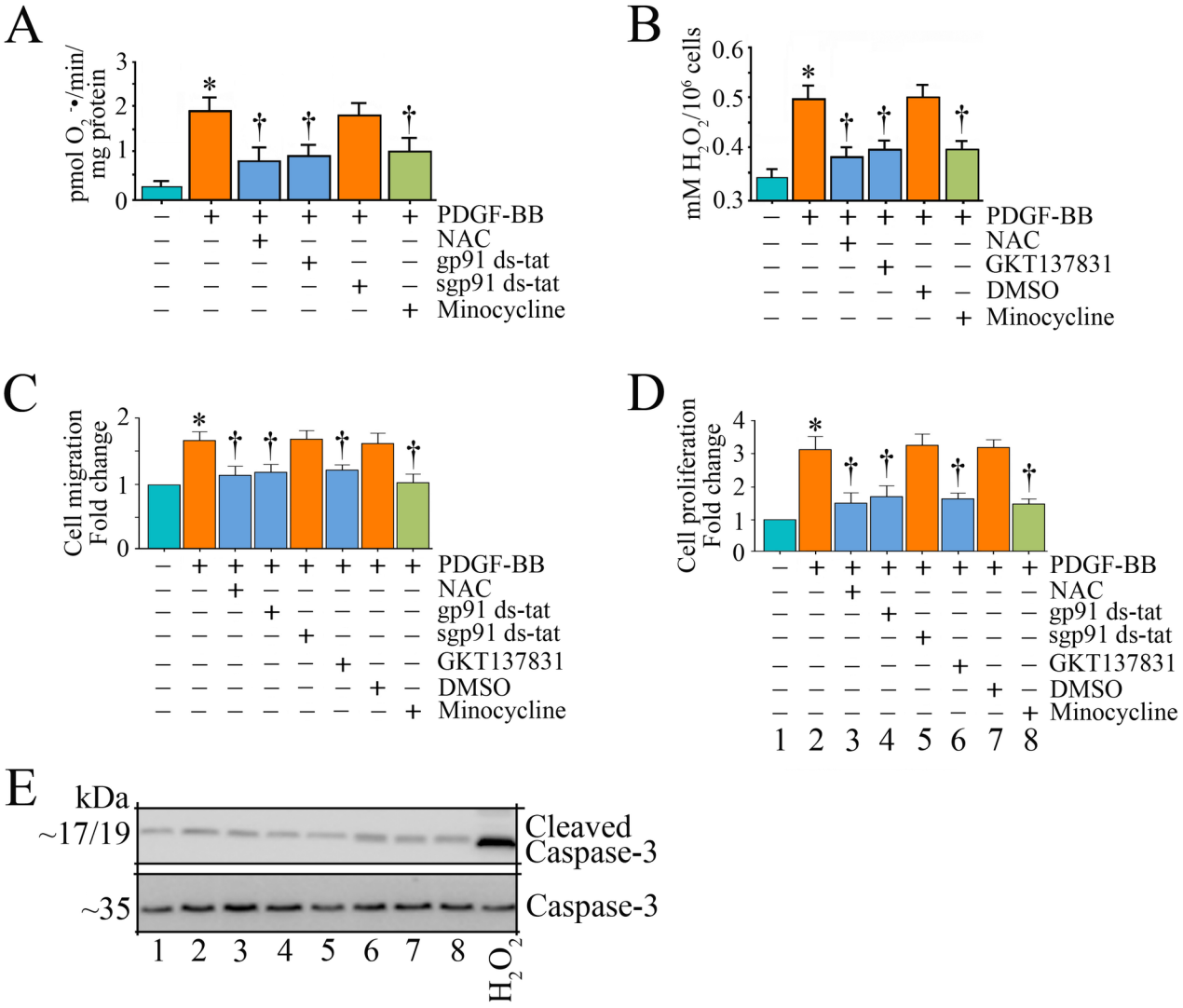
A
pmol O2 •−/min/ mg pfotein
PDGF-BB
NAC
gp91 ds-tat
sgp91 ds-tat
Minocycline
B
mM H2O2/10^6 cells
PDGF-BB
NAC
GKT137831
DMSO
Minocycline
C
Cell migration Fold change
PDGF-BB
NAC
gp91 ds-tat
sgp91 ds-tat
GKT137831
DMSO
Minocycline
D
Cell proliferation Fold change
PDGF-BB
NAC
gp91 ds-tat
sgp91 ds-tat
GKT137831
DMSO
Minocycline
1 2 3 4 5 6 7 8
E
kDa
~17/19
Cleaved Caspase-3
~35
Caspase-3
1 2 3 4 5 6 7 8
H2O2

Figure 3

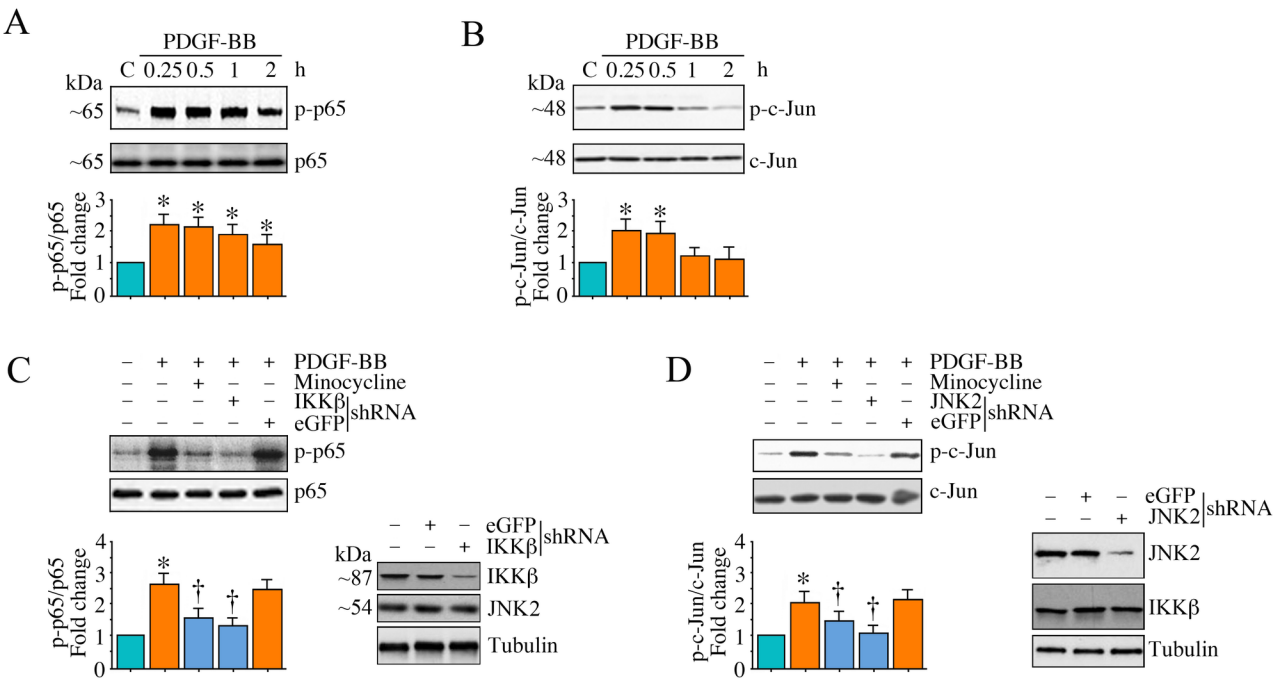
A
PDGF-BB
C 0.25 0.5 1 2 h
kDa
~65
p-p65
~65
p65
p-p65/p65
Fold change
B
PDGF-BB
C 0.25 0.5 1 2 h
kDa
~48
p-c-Jun
~48
c-Jun
p-c-Jun/c-Jun
Fold change
C
PDGF-BB
Minocycline
IKKβ|shRNA
eGFP|shRNA
p-p65
p65
p-p65/p65
Fold change
eGFP|shRNA
IKKβ|shRNA
kDa
~87
IKKβ
~54
JNK2
Tubulin
D
PDGF-BB
Minocycline
JNK2|shRNA
eGFP|shRNA
p-c-Jun
c-Jun
p-c-Jun/c-Jun
Fold change
eGFP|shRNA
JNK2|shRNA
JNK2
IKKβ
Tubulin

Figure 4

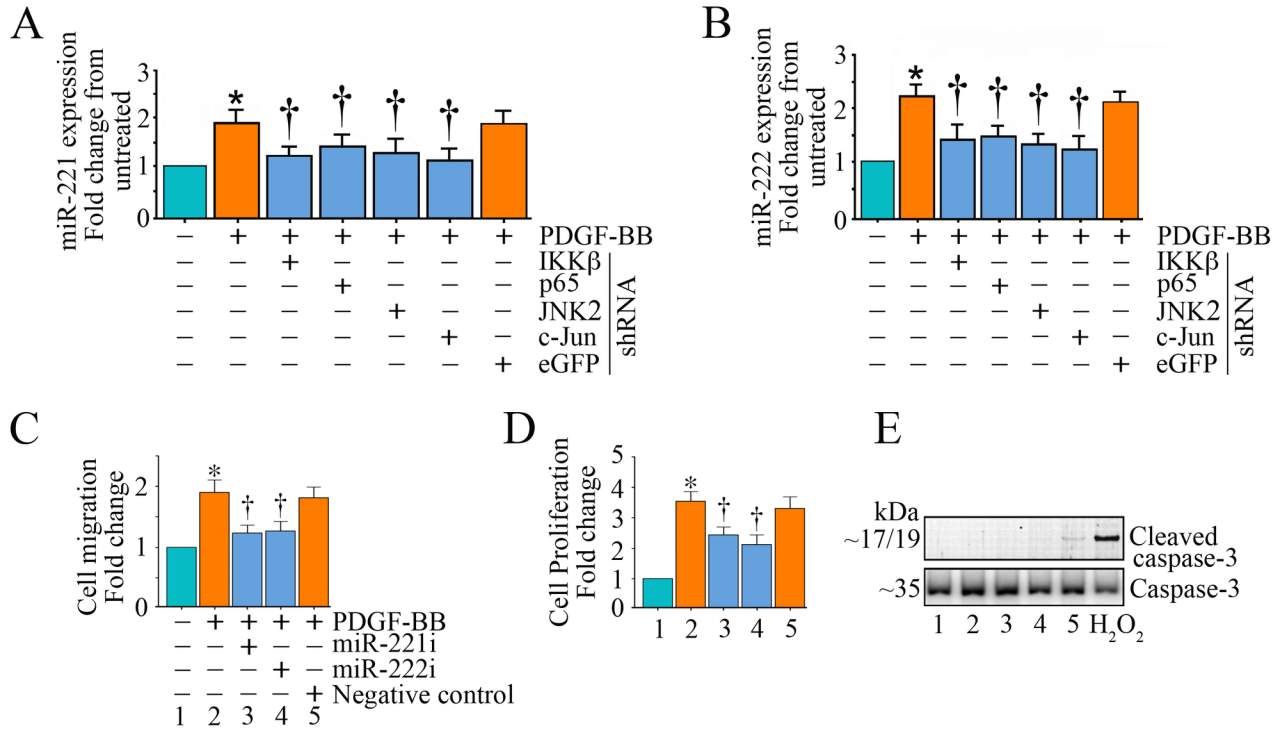
A
miR-221 expression
Fold change from untreated
PDGF-BB
IKKβ
p65
JNK2
c-Jun
eGFP
shRNA
B
miR-222 expression
Fold change from untreated
C
Cell migration
Fold change
miR-221i
miR-222i
Negative control
D
Cell Proliferation
Fold change
E
kDa
~17/19
Cleaved caspase-3
~35
Caspase-3
H2O2

Figure 5

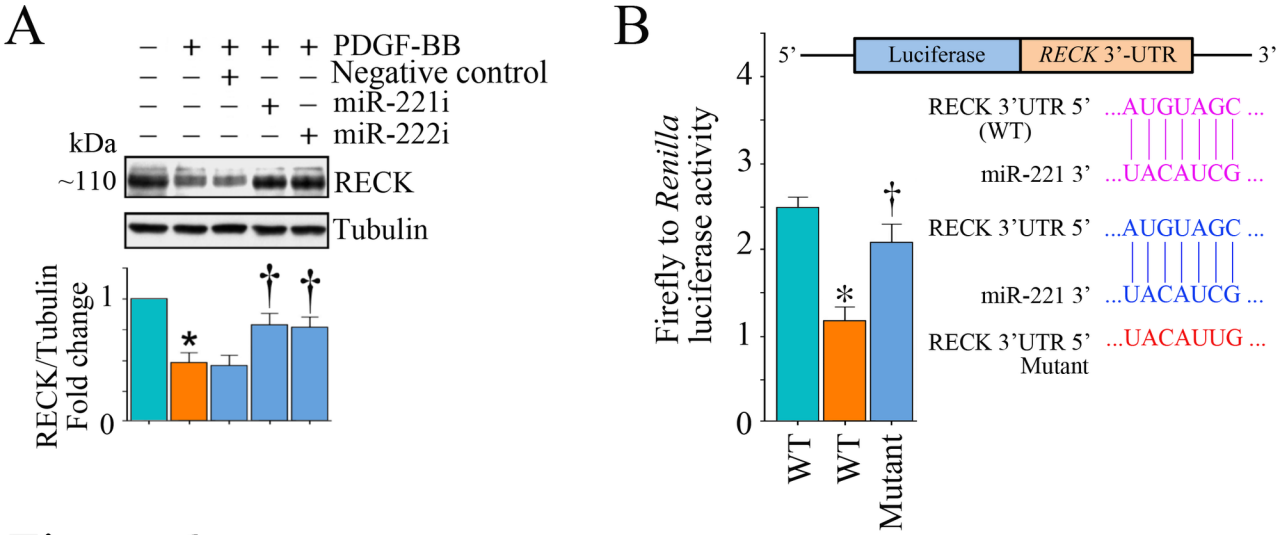
A
PDGF-BB
Negative control
miR-221i
miR-222i
kDa
~110
RECK
Tubulin
RECK/Tubulin
Fold change
B
5'
Luciferase
RECK 3'-UTR
3'
Firefly to Renilla
luciferase activity
RECK 3'UTR 5'
(WT)
...AUGUAGC ...
miR-221 3'
...UACAUCG ...
RECK 3'UTR 5'
...AUGUAGC ...
miR-221 3'
...UACAUCG ...
RECK 3'UTR 5'
Mutant
...UACAUUG ...
WT
WT
Mutant
PDGF-BB

Figure 6

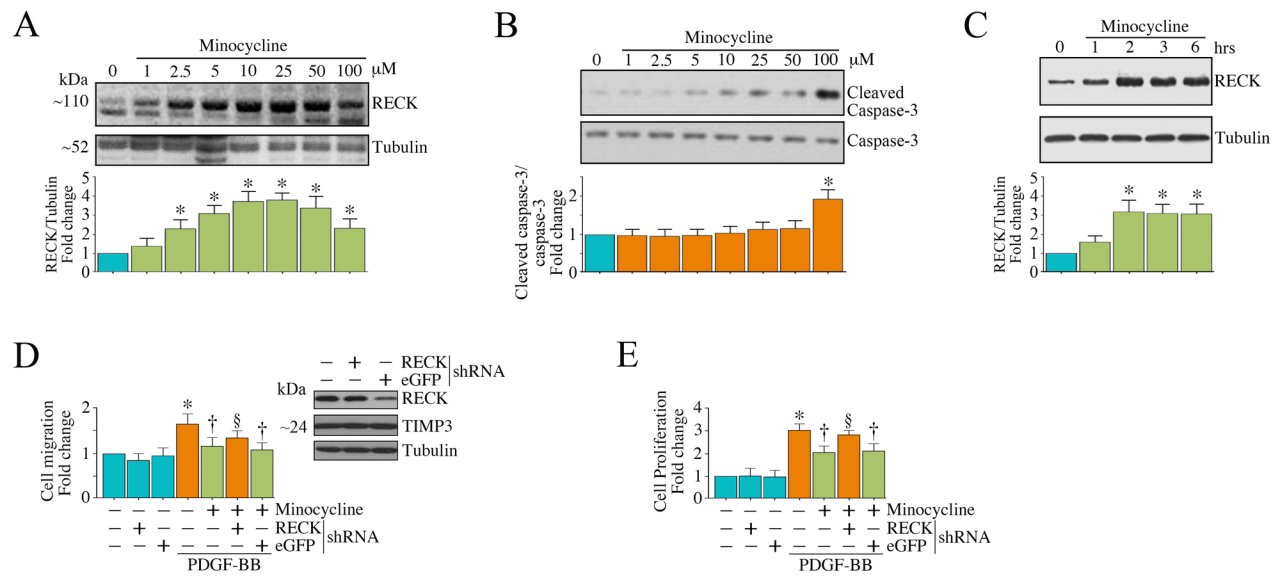
A
Minocycline
0 1 2.5 5 10 25 50 100 μM
kDa
~110
RECK
~52
Tubulin
RECK/Tubulin Fold change
B
Minocycline
0 1 2.5 5 10 25 50 100 μM
Cleaved Caspase-3
Caspase-3
Cleaved caspase-3/ caspase-3 Fold change
C
Minocycline
0 1 2 3 6 hrs
RECK
Tubulin
RECK/Tubulin Fold change
D
RECK
eGFP
shRNA
kDa
RECK
~24
TIMP3
Tubulin
Cell migration Fold change
Minocycline
RECK
eGFP
shRNA
PDGF-BB
E
Cell Proliferation Fold change
Minocycline
RECK
eGFP
shRNA
PDGF-BB

Figure 7

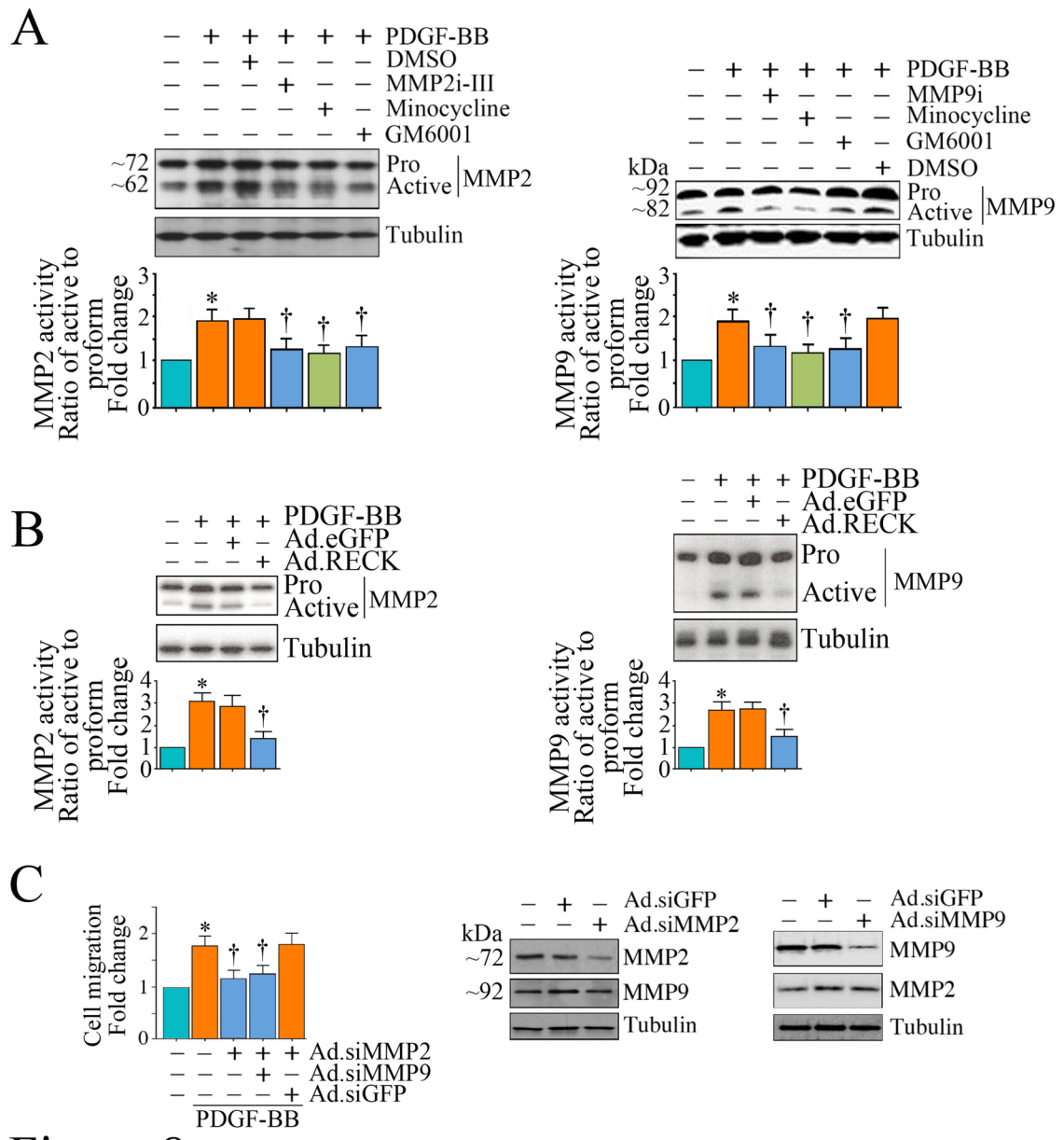
A
PDGF-BB
DMSO
MMP2i-III
Minocycline
GM6001
~72
~62
Pro
Active
MMP2
Tubulin
MMP2 activity
Ratio of active to proform
Fold change
MMP9i
kDa
~92
~82
MMP9
B
Ad.eGFP
Ad.RECK
C
Cell migration
Fold change
Ad.siMMP2
Ad.siMMP9
Ad.siGFP

Figure 8

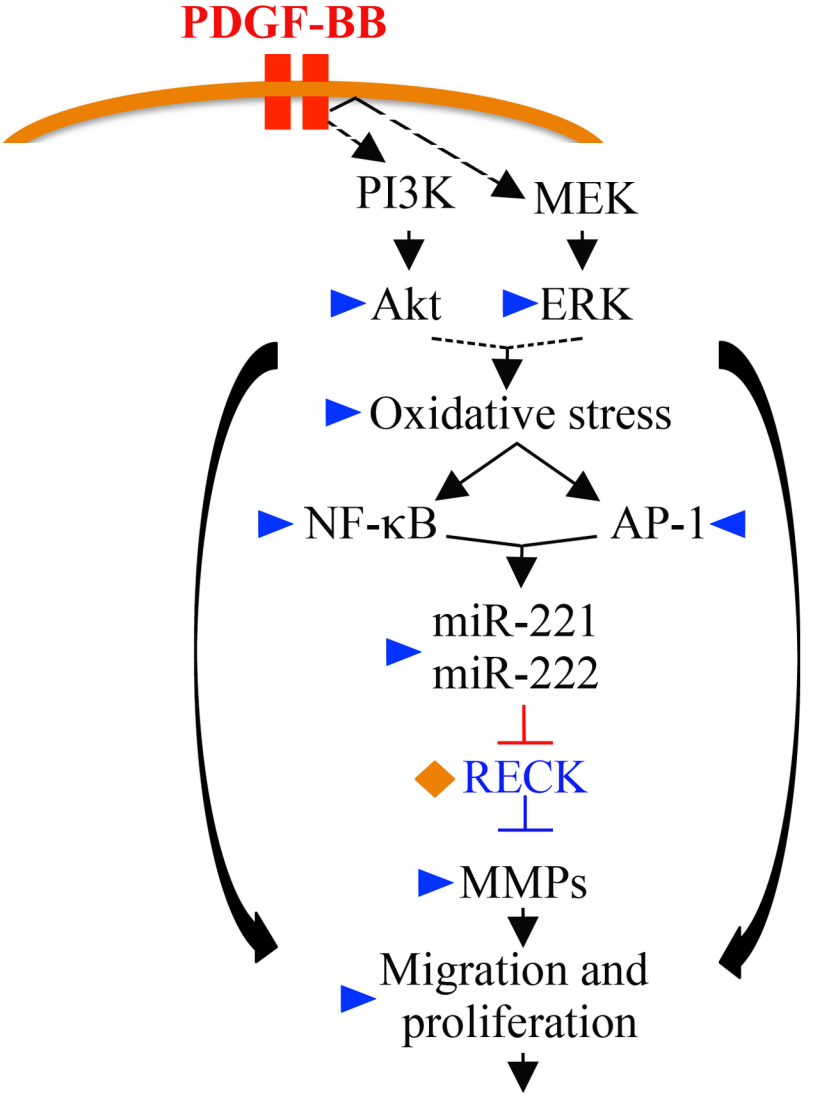
PDGF-BB
PI3K
MEK
Akt
ERK
Oxidative stress
NF-κB
AP-1
miR-221
miR-222
RECK
MMPs
Migration and
proliferation
Vascular proliferative diseases

Figure 9